Eur. Phys. J. Appl. Phys. (2014) 66: 20104
DOI: 10.1051/epjap/2014130470

The European Physical Journal Applied Physics

Regular Article

ZnO/PS/p-Si heterojunction properties

Uday Muhsin Nayef, Mohammed Waleed Muayad[a], and Haider Amer Khalaf

Department of Applied Science, University of Technology, 9183 Baghdad, Iraq

Received: 15 October 2013 / Received in final form: 5 March 2014 / Accepted: 2 May 2014
Published online: 5 June 2014 – © EDP Sciences 2014

Abstract. In this paper porous silicon (PS) has been prepared by electrochemical etching technique and then ZnO thin film deposition on PS by spray pyrolysis method, the study of AFM show improve the structural stability of the PS substrate with crystalline growth of ZnO thin film. PL spectra explained a blue-shifting in PS layer come from oxidation the surface of PS after coating with ZnO film, Raman measurement show quantum confinement in PS layers with decreasing in variation mode of ZnO film, and the *J-V* characteristic show increasing in resistivity of Al/ZnO/PS/*c*-Si/Al due to increasing in depletion layer junction compere with PS layer.

1 Introduction

Nanotechnology has gained substantial popularity recently due to the rapidly Developing techniques both to synthesize and characterize materials and devices at the nanoscale (1–100 nm) [1]. The research in the field of zinc oxide/porous silicon (ZnO/PS) has attracted much attention within community as a modern material because of an increasing requires for short-wavelength photonic devices, high power and high frequency electronic devices and full cell. Where PS materials can have index large photoluminescence (PL) efficiency at room temperature in the visible flexibility to control and the potential applications in Si-based optoelectronic [2] and PS has since the PL Efficiency of bulk silicon is very low, due to its indirect energy band gap and short nonradiative lifetime. The reason of this was the partial dissolution of silicon [3].

ZnO is a II–VI compound semiconductor with wide direct band-gap energy $E_g = 3.37$ eV that is suitable for short-wavelength optoelectronic applications and the high excitation binding energy 60 MeV in ZnO crystal can ensure efficient excitonic emission at room temperature. ZnO is transparent to visible light and can be made high conductive by doping and its diverse growth morphologies make ZnO a key material in the field of nanotechnology and wide band-gap semiconductors [4]. When ZnO thin film deposition on silicon substrate has received increasing interest for their lower cost and larger size. Unfortunately, the large mismatches in the lattice constant and thermal expansion coefficients would introduce a slightly large stress between the ZnO and Silicon substrate. On the other hand, the sponge-like open structure and large specific surface area make PS nanostructures a suitable material for accommodating ZnO into its pores and thus establishing a good nucleation site which is essential for the growth along the preferred orientation [5]. Due to their excellent characteristic, PS nanostructures was used as a substrate to growth nanostructures materials such as ZnO nanostructures and carbon nanotubes.

2 Experimental work

Experimental work consist prepared porous silicon by electrochemical anodization etching of *p*-type silicon $\langle 1\,1\,1 \rangle$ oriented with a resistivity 1.5–4 Ω cm and the etching cell made from teflon because the teflon not interaction with HF acid, rubber O-ring is used before the upper part of cell. The latter has a central circular of 1 cm^2 to allow touching the silicon wafer. And the two electrodes are used to apply current across the cell. The lower one is stainless still foil below silicon wafer and the upper one is gold mesh connected with the HF solution as shown in Figure 1. And after etching process, the sample were rinsed with ethanol and pentane and dried by nitrogen. After prepared PS samples, After that porous silicon layer coating by ZnO thin film 200 nm thickness by thermal spray pyrolysis with substrate temperature 400 °C and spray rate 3 mL min^{-1} and deposition rate 100 nm min^{-1} and gas pressure 2 bar. Study morphological properties the effect of coating by AFM the atomic force micrographs were taken for sample by AA3000 scanning probe microscope Angstrom Advanced Inc. before and after coating, structure properties of ZnO/PS at characterized by XRD-6000 Shimadzu Japan, electrical properties *J-V* and *C-V* measurements of PS and PS/ZnO after deposition ohmic contact by thermal evaporation.

[a] e-mail: mwaleed1987@gmail.com

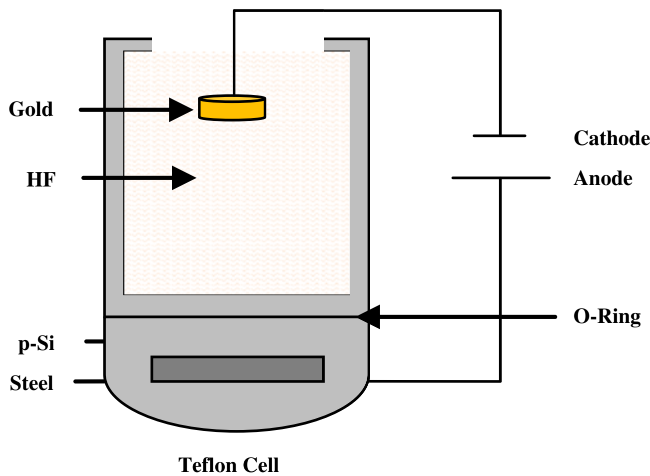

Fig. 1. Electrochemical etching cell.

Table 1. AFM calculation of PS, ZnO and ZnO/PS.

Sample type	Average grain diameter (nm)	Roughness (nm)
PS	33.80	0.970
ZnO	105.3	0.314
ZnO/PS	85.21	0.894

3 Results and discussions

3.1 Morphology properties

Figure 2 showing the morphology of porous silicon after coating by ZnO thin film, ZnO partially filling or completely covering pores. The surface of the PS layer is a sponge-like structure which consists of large number of pores and voids. These pores and voids make porous silicon an adhesive surface for accommodating ZnO into its pores. Thus, the ZnO thin film acted as a transparent capping and providing a good coverage of the crystallite surface on the PS substrate (Fig. 2c), which could improve the structural stability of the PS substrate [7] and also in Figure 2c the average grain diameter of ZnO particle decreasing when deposition on PS surface because PS surface act as nucleation sites, which induced ZnO to grow along the preferred orientation.

3.2 Structure properties

Figure 3 showing XRD patterns of ZnO/PS, the ZnO/PS layers exhibited a dominant diffraction peak at $2\theta = 28.3825$, corresponding to the PS (1 1 1) layer. The diffraction peak at (31.8744, 346070, 36.4616) corresponds to the (1 0 0, 0 0 2, 1 0 1) plane of the ZnO film, which indicates that the ZnO thin film was highly oriented along the c-axis vertical to the PS layer [8]. The broadening of the (FWHM) of the diffraction peak of the PS (1 1 1) layer was estimated from XRD. The sharp diffraction peak from the ZnO film with a weak FWHM indicates the high quality of the ZnO film [9]. The strain ($\in$ %) of the nanocrystalline

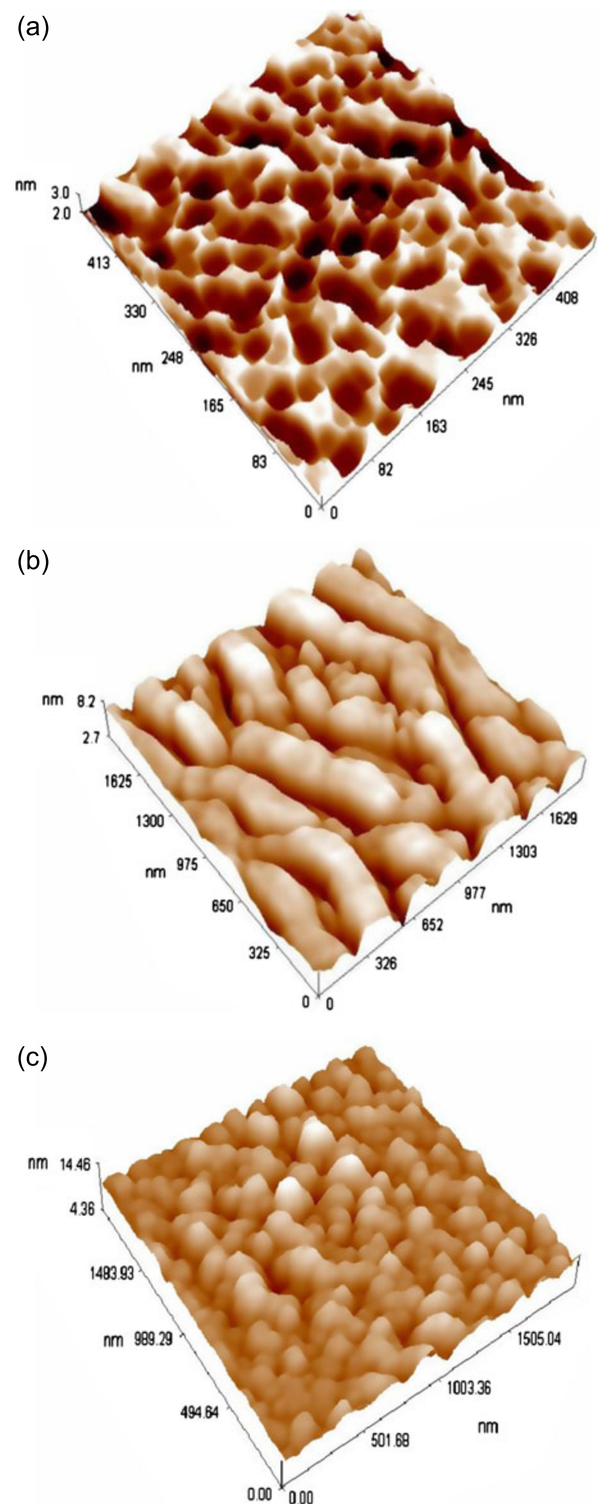

Fig. 2. AFM image of (a) PS (b) ZnO deposition on glass (c) ZnO thin fim deposition on porous silicon layer.

ZnO film grown on the PS layer along the c-axis can be calculated using the following equation:

$$\text{Micros strain } (\in \%) = \frac{c - c_0}{c_0}, \tag{1}$$

Table 2. Calculation of XRD spectral of ZnO/PS.

Material	2θ (deg.)	$h\,k\,l$	FWHM (deg.)	a (nm)	c (nm)	d (nm)	L (nm)
PS⟨1 1 1⟩	28.382	101	2.0559	0.536	–	0.31	4.00
ZnO	31.874	100	1.0667	0.3381	–	0.28	7.78
	34.607	002	1.0375	–	0.5179	0.25	8.05
	36.461	101	1.0500	0.3381	0.5179	0.24	7.99

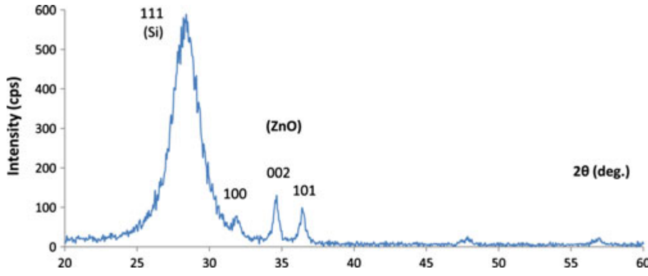

Fig. 3. XRD of ZnO/PS.

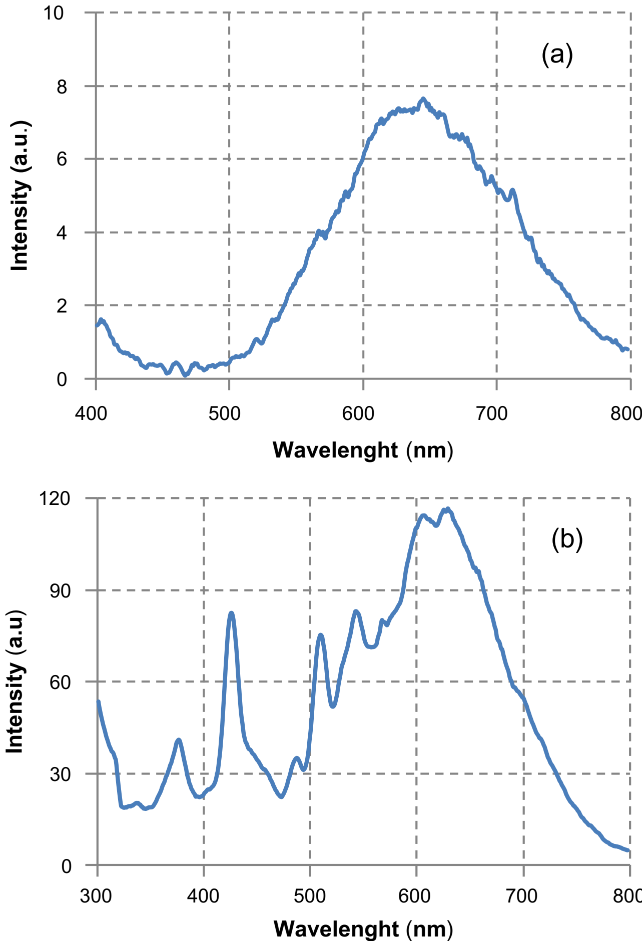

Fig. 4. PL of (a) PS and (b) ZnO/PS.

Table 3. PL emission of PS and ZnO/PS.

Sample type	Wavelength (nm)	Energy gap (eV)
PS	644.2	1.92
ZnO/PS	368.1	3.37
	452.1	–
	524.6	–
	548.9	–
	628.3	1.975

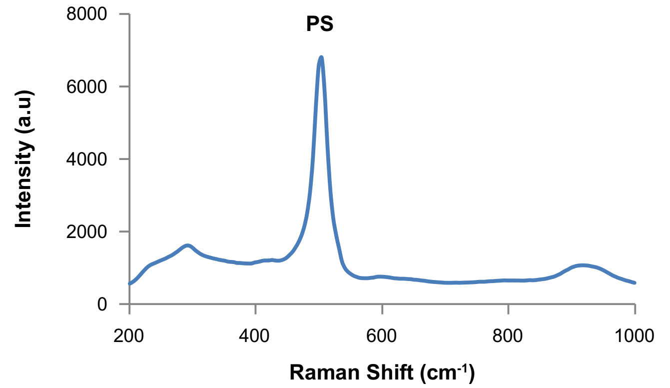

Fig. 5. Raman spectrum of ZnO/PS.

where c is the lattice constant of the strained ZnO film calculated from XRD data by using equations (1) and (2) and c_0 is the unstrained lattice constant for ZnO_2. The lattice constants for hexagonal ZnO film are reported in JCPDS standard data $a_0 = 3.24982$ Å and $c_0 = 5.20661$ Å.

$$\frac{1}{d^2} = \frac{4}{3} \times \left(\frac{h^2 + hk + k^2}{a^2}\right) + \frac{l^2}{c^2}, \qquad (2)$$

where a and c are the lattice constants of ZnO.

The obtained value of strain is -0.517%. A negative value is associated with compression strain. The low value of the compression strain revealed that the ZnO film referred to grow along the c-axis, and gave evidence of a high-quality crystal resulting.

3.3 Photoluminescence

PL spectra of ZnO/PS layers (Fig. 4) show that the boarding peck near 630 nm revealing the good quality of the PS layers, that the blue shift in PS is attributed to quantum confinement effects of electrons in nanosized particles in PS layers and the decreasing of emission wavelength of PS layers after ZnO deposition is related that the surface oxidation by ZnO and this increasing the energy gap of PS (Tab. 3), the peak 368 nm (UV emission) is due

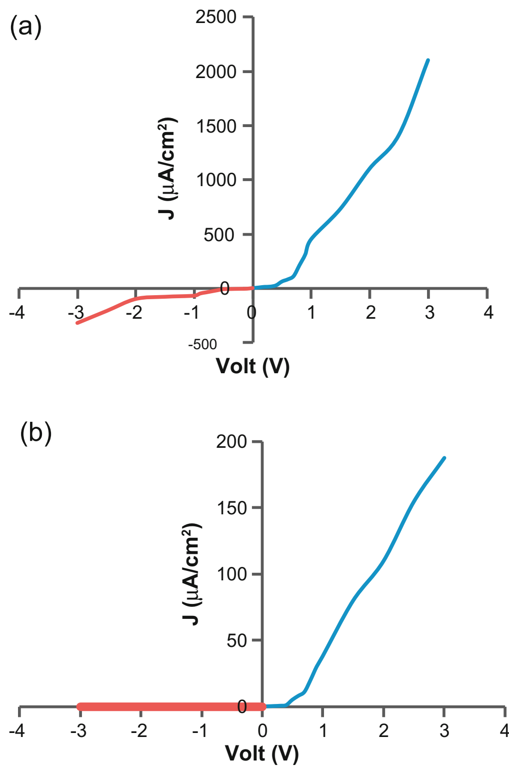

Fig. 6. *J-V* characteristic of (a) PS and (b) ZnO/PS.

to the near band emission (NBE) in the wide band gap of ZnO from the direct recombination of the photo-generated charge carrier or recombination of free exactions through an exciton-exciton collision process [8,9].

Figure 5 show Raman scattering spectrum of ZnO/PS, the shapes peaks at approximately 520 cm^{-1} refer to first – order scattering phonons in *c*-Si and this characterized the PS layers and This feature of Si nanocrystals is attributed to the quantum confinement of optical phonons in the electronic wave function of Si nanocrystalsthe low frequency come from optical phonon confinement in Si nanocrystals [10]. The observed phonon frequency at 305 cm^{-1} was also related to the *c*-Si substrate in the ZnO/PS layers.

3.4 Electrical measurement

3.4.1 J-V characteristic

When porous silicon coating by ZnO thin film we note more decreasing in output current due to increasing resistivity that come from increasing in depletion width of the sandwich structure (Al/ZnO/PS/*c*-Si/ZnO). That the forward and reverse bias Al/ZnO/PS/*p*-Si/Al responded double Schottky heterojunction. And these junctions will increase the resistivity of layers. It can be noticed from this figure that the junction exhibits rectifying behavior. This rectifying behavior is attributed to heterojunction potential barrier at the ZnO/PS interface. The formation of the heterojunction structure is referred to the difference in energy gap between the ZnO and PS.

3.4.2 C-V characteristic

A *C-V* characteristic is a technique for characterizing semiconductor materials and devices. The applied voltage is varied, and the capacitance is measured and plotted as a function of voltage as shown in Figure 7. The depletion region with its ionized charges inside behaves like a capacitor. The *C-V* measurement show decreasing in capacitance more than PS only this due to large increasing in resistivity of sandwich structure of (Al/ZnO/PS/*c*-Si/Al)

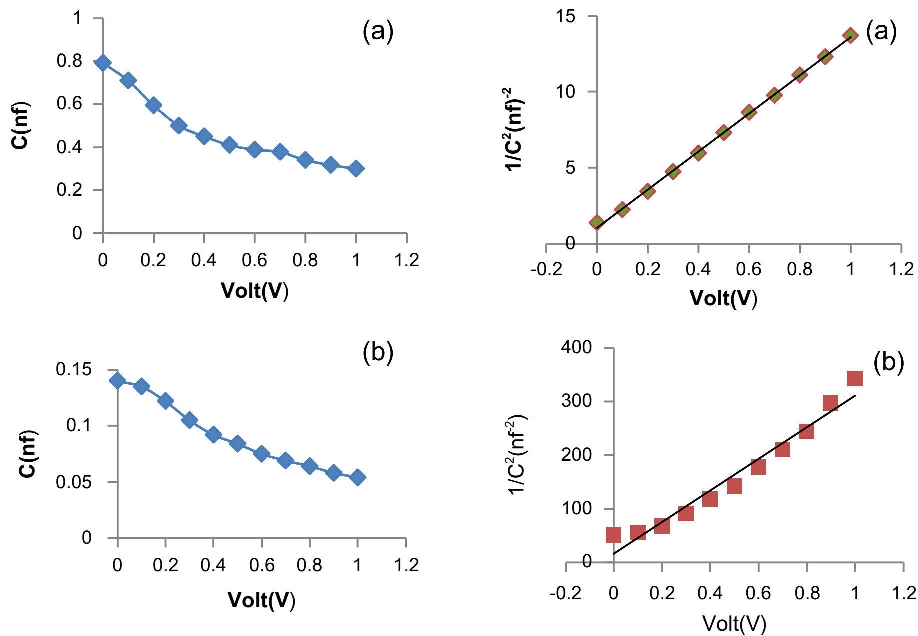

Fig. 7. The *C-V* characteristics of (a) Al/PS/*c*-Si/Al and (b) Al/ZnO/PS/*c*-Si/Al.

Table 4. The value of built up potential, effective charge carrier, and width of depletion layers of ZnO/PS samples.

Sample type	N_{d} (cm^{-3})	W (μm)	V_{bi} (volt)
PS	2.2×10^{12}	3.25	0.181
ZnO/PS	1.2×10^{11}	15.3	0.09

and increasing in width of depletion layer (Tab. 4) because filling of pores of PS with ZnO practical.

4 Conclusion

After deposition ZnO on PS layer the surface stability of PS increasing with increasing in boarding in XRD spectra of PS, PL spectra of ZnO/PS show that increasing in blue shifting in PS layers after ZnO deposition related that the surface oxidation by ZnO, and the increasing UV-emission of ZnO come from direct recombination of the photogenerated free carrier. Raman scattering referred multiphonons processes in ZnO/PS, also the resistivity of Al/ZnO/PS/*c*-Si/Al due to increasing in depletion layer junction compere with PS layer.

References

1. M. Kohler, W. Fritzsche, *Nanotechnology* (Wiley-VCH, Weinheim, Germany, 2004)
2. R. Smith, S. Collins, J. Appl. Phys. **71**, R1 (1992)
3. O. Bisi, S. Ossicini, L. Pavesi, Surf. Sci. Rep. **38**, 1 (2000)
4. M. Basak, Mater. Res. Bull. **42**, 875 (2007)
5. R.G. Singh, F. Singh, V. Agarwal, R.M. Mehra, J. Phys. D **40**, 3090 (2007)
6. S.S. Fan, M.G. Chapline, N.R. Franklin, T.W. Tombler, A.M. Cassell, H.J. Dai, Sci. J. **283**, 512 (1999)
7. S.M. Thahab, Opt. Adv. Mat. **5**, 1107 (2011)
8. N. Izni , M. Tankikawa, M.R. Mahmood, K. Yasui, A.M. Hashim, Mater. J. **5**, 2817 (2013)
9. K.A. Salman, K. Omar, Z. Hassan, Sol. Energy J. **86**, 541 (2011)
10. A.V. Lartsev, I.A. Gayduchenko, V.Y. Timoshenko, Microelectron. Eng. J. **90**, 96 (2012)